Experiments on Pilot Symbol-Assisted Coherent Multistage Interference Canceller for DS-CDMA Mobile Radio

Mamoru Sawahashi, *Member, IEEE,* Kenichi Higuchi, Hidehiro Andoh, and Fumiyuki Adachi, *Fellow, IEEE*

***Abstract*—A three-stage coherent multistage interference canceller (COMSIC) employing pilot symbol-assisted (PSA) channel estimation for replica generation of multiple access interference (MAI) is implemented and its performance in the presence of frequency selective multipath fading is experimentally evaluated by a multipath fading simulator. A fast transmission power control (TPC) method suitable for COMSIC is also proposed, in which the signal-to-interference plus background noise power ratio (SIR) at the matched filter (MF) based Rake receiver is measured to achieve a short TPC delay and the target signal-to-interference ratio value is compensated by an outer loop so that the measured block error rate (BLER) is equal to the prescribed target value. The experimental results show that as expected the COMSIC satisfactorily reduces the MAI even when the number of active users is equal to the spreading factor in a multipath fading environment, and thus, improves the bit error rate (BER) performance in a multiuser environment. The results also show that the proposed fast TPC method with a two-slot delay associated with COMSIC works satisfactorily and the combination of COMSIC and fast TPC significantly decreases the transmission power of a mobile station (required transmission power of a mobile station with COMSIC at the average BER of 10^{-3} is decreased by approximately 2.0 (3.0) dB compared with the MF-based Rake receiver with (without) antenna diversity reception). This extends the cell coverage, battery life, and increases the system capacity in the reverse link.**

***Index Terms*—Channel estimation, direct sequence-code division multiple access, interference canceller, transmission power control.**

I. Introduction

AFTER enthusiastic efforts for standardization in the third-generation partnership project (3GPP) and development of wideband direct sequence-code division multiple access (W-CDMA) [1], [2], commercial W-CDMA service has just been launched, in Japan, in May of last year. In W-CDMA, all users communicate simultaneously in the same frequency band and, hence, multiple access interference (MAI) is the major cause of transmission impairment [3], [4]. In mobile radio, since the received signal is subjected to multipath fading according to the movement of a mobile station (MS) as well as distance-dependent path loss and shadowing, a high degree of MAI is often produced, which significantly degrades the reverse link performance. Furthermore, in multimedia mobile communications offered by, for example, the IMT-2000 system [5], data rates may vary widely and high rate users may produce severe MAI in the reverse link. Employing an interference canceller or multiuser detection [6], [7] is a promising method for decreasing the severe MAI especially from high-data rate users, thereby significantly reducing the transmission power of the MS in the reverse link. A multistage interference canceller [8]–[13] is popular and suitable for practical implementation because interference suppression is achieved at a reasonable level of complexity. However, in order to apply the multistage interference canceller to multipath fading environments, where the received phase and amplitude randomly vary, accurate channel estimation is required for precise replica generation of the MAI. Thus, we proposed the pilot symbol-assisted (PSA) coherent multistage interference canceller (COMSIC) in which channel estimation using pilot symbols of each user is successively performed after MAI cancellation at each stage, resulting in the accurate generation of interference replicas [11]. It was also reported that the link capacity in an isolated cell is increased by approximately two times that of the matched filter (MF)-based Rake receiver [13]. Recently, many theoretical analyses have been reported approximating MAI by Gaussian noise and computer simulation evaluations assuming ideal chip synchronization except for some studies. In [14] and [15], the impact of estimation errors of the resolved path timing on the performance of the decorrelating receiver or minimum mean square error (MMSE) multiuser receiver are numerically analyzed. However, their approaches are based on statistical analysis assuming the additive white Gaussian noise (AWGN) channel, with a near-infinite dynamic range of the received signal representation (note that this assumption is advantageous to an actual interference canceller and multiuser operations). Nevertheless, in a real multipath fading channel, estimation errors of the resolved path timing occur when the received signal level drops with a burst property similar to the decided bit errors. Thus, the investigation of an interference canceller taking into account path search, i.e., chip synchronization for filtered signals in a multipath fading channel is needed aiming at actual system applications. Furthermore, most studies thus far have not focused on the effect of the interference canceller associated with fast transmission power control (TPC), which is an essential technique in the direct sequence-code division multiple access (DS-CDMA) reverse link to avoid the near–far problem, assuming a reasonable quantization of the received signal.

Manuscript received December 24, 2000; revised August 3, 2001.

M. Sawahashi, K. Higuchi, and H. Andoh are with the Wireless Access Laboratory, NTT DoCoMo, Inc., Kanagawa-ken 239-8536, Japan (e-mail: sawahasi@mlab.yrp.nttdocomo.co.jp).

F. Adachi is with the Department of Electrical and Communication Engineering, Graduate School of Engineering, Tohoku University, Sendai-shi, Miyagi 980-8579, Japan.

Publisher Item Identifier S 0733-8716(02)00993-9.

TABLE I
EXPERIMENTAL SYSTEM PARAMETERS

Chip rate (Bandwidth)		1.024 Mcps (1.25 MHz)
Carrier rate		64 ksps
Information bit rate		32 kbps
Processing gain		16 × 0.5 × 3
Modulation	Data	QPSK
	Spreading	QPSK
Channel model		Equal average power L-path Rayleigh fading
Channel estimation		Pilot symbol-assisted channel estimation (2-slot averaging)
Channel coding		Convolutional coding (R = 1/3, k = 7) / Soft-decision Viterbi decoding
Diversity		2-branch antenna diversity/ Max. 4-finger Rake diversity
Maximum number of stages		3

Therefore, this paper elucidates the effect of a three-stage COMSIC employing PSA channel estimation [16]–[20] for replica generation of MAI, which we implemented, in frequency-selective multipath fading channels by laboratory experiments. The implemented PSA-COMSIC (we call simply COMSIC hereafter) receiver has the analog-to-digital (A/D) converter quantization of 8 bits and an automatic gain control (AGC) amplifier with the dynamic range of approximately 70 dB. By using the COMSIC at a base station (BS) receiver, MAI and multipath interference (MPI) in the reverse link are effectively decreased. However, in an actual cellular system application in a multicell configuration, the combination of COMSIC and fast TPC is indispensable in order to decrease the interference to other cells, i.e., increase system capacity. In general, COMSIC accompanies the processing delay beyond an interval of several slots especially when the number of active users, K, is large. Even for the parallel-type COMSIC, in which channel estimation, data decision, and MPI replica generation are performed simultaneously at the same stage, a long processing delay proportional to the number of stages is required. Thus, we also propose a SIR measurement based fast TPC method suitable for COMSIC that can be achieved with a two-slot delay and experimentally investigate the combined effect of COMSIC and fast TPC. This paper is organized as follows. Section II describes the experimental receiver with COMSIC and the fast TPC method for COMSIC. After briefly describing the experimental configuration, experimental results using COMSIC without and with fast TPC are discussed in Section III.

II. EXPERIMENTAL COMSIC RECEIVER

A. Received Signal Representation

Before describing the experimental COMSIC receiver, the received signal representation is given in order to provide a thorough understanding of how the MAI cancellation is performed in the receiver. The major radio link parameters used in the experiments are given in Table I. The 32-kbps original data sequence was first segmented into blocks of 378-bit data (tail bits and dummy bits were included to fill the frames completely). Twelve-bit cyclic redundancy check (CRC) parity bits are calculated for the block-wise data bits for convolutional coding. After applying the channel coding of a one-third rate convolutional code with a constraint length of 7 bits (its generator polynomials are 554, 624, and 764 in octal notation), the coded data of 1,152 bits were block interleaved using a 72×16-bit interleaver. After adding dummy bits, eight pilot bits required for coherent channel estimation and TPC bits were time-multiplexed, the coded data sequence was transformed into a QPSK symbol sequence with 64 ksymbol/s (ks/s). One frame comprised 16 slots each with the length of 0.625 ms and one slot consisted of $N_p = 4$ pilot symbols and $N_s = 36$ coded data symbols including TPC and dummy symbols. The transmission power of the pilot symbols was set to be identical to that of the coded data symbols. The optimum number of pilot symbols within a slot, N_p, was derived from the tradeoff between improving the channel estimation and decreasing the frame efficiency. The parameter $N_p = 4$ symbols was optimized by computer simulation [18]. The symbol sequence of each data channel was multiplied with an orthogonal-gold sequence with the repetition period of 64 chips and a scrambling code with the repetition period of 2^{41} chips. Therefore, the spreading factor (SF) is 16 and the processing gain becomes $P_g = 16 \times 0.5 \times 3 = 24$, where the factor of three is the SF due to convolutional coding. The spreading chip rate was 1.024 Mcps. To confine the spread signals within the bandwidth of 1.25 MHz, a square-root raised cosine Nyquist transmission filter with the rolloff factor of 0.22 was applied before frequency conversion into the carrier frequency of 1990.5 MHz and power amplification.

Let $d_k(t)$ and $c_k(t)$ be the QPSK modulated signal waveform and spreading waveform of the kth user, respectively. They are represented as $d_k(t) = \sum_{i=-\infty}^{\infty}[\exp j\phi_k(i)]u(t/T - i)$ and $c_k(t) = \sum_{i=-\infty}^{\infty} a_k(j)u(t/T_c - i)$, where $a_k(j)$ represents the random, binary, long scrambling sequence with $|a_k(j)| = 1, \phi_k(i) \in \{m\pi/2; m = 0 - 3\}$ is the QPSK modulation phase, T and T_c are the QPSK symbol duration and chip duration, respectively, $u(t) = 1(0)$ for $0 \le t < 1$ (otherwise), and $\mathrm{SF} = T/T_c$ represents the spreading factor. The transmitted spread signal, $d_k(t)c_k(t)$, of the kth user propagates through a multipath channel. Assuming L_k discrete propagation paths, the received composite signal $r^{(b)}(t)$ at bth antenna $(1 \le b \le 2)$, is represented as

$$r^{(b)}(t) = \sum_{k=1}^{K}\sum_{l=1}^{Lk} \xi_{k,l}^{(b)}(t) d_k(t - \tau_{k,l}) c_k(t - \tau_{k,l}) + n^{(b)}(t)$$
$$= \sum_{k=1}^{K}\sum_{l=1}^{Lk} I_{k,l}^{(b)}(t - \tau_{k,l}) + n^{(b)}(t) \quad (1)$$

where, $\xi_{k,l}^{(b)}(t)$ and $\tau_{k,l}(t)$ are the complex gain and the time delay of the lth path $(1 \le l \le L_k)$ associated with the kth user at bth antenna, respectively, K is the number of active users and $n^{(b)}(t)$ is the additive Gaussian noise component at bth antenna with one-sided spectral density N_0. It is assumed that $\sum_{l=1}^{Lk} E|\xi_{k,l}(t)|^2 = 2P_k$, where $E[\cdot]$ denotes the ensemble average and P_k is the average received power.

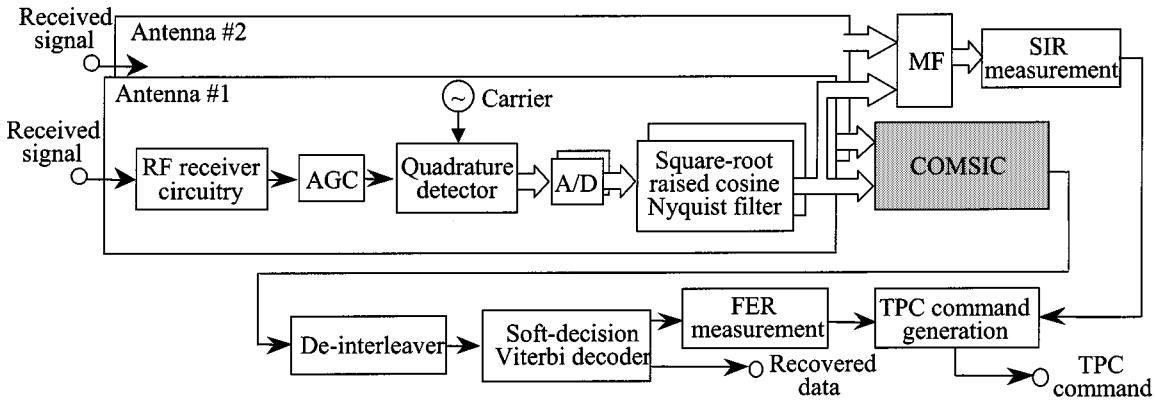

Fig. 1. Block diagram of PSA-COMSIC receiver.

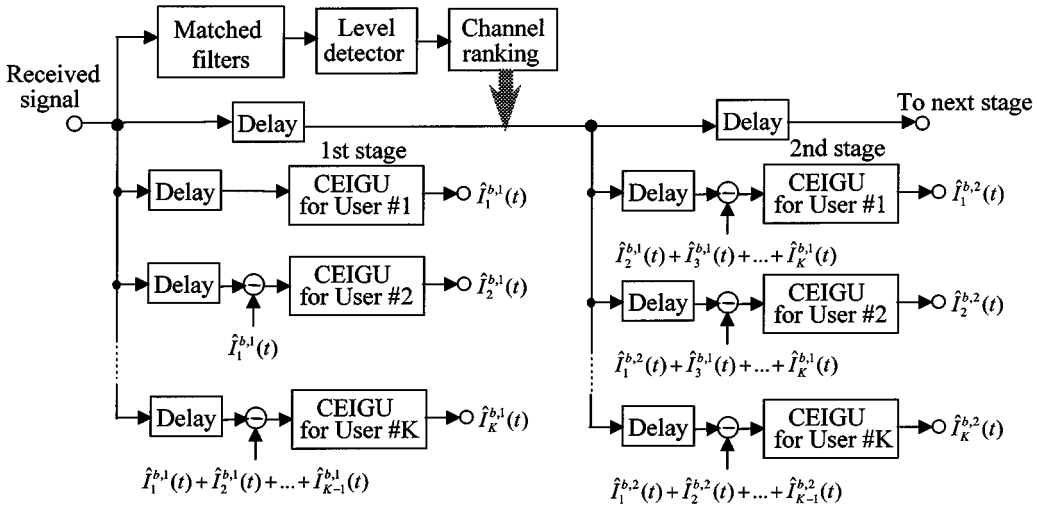

Fig. 2. COMSIC structure (for bth antenna branch $(b = 1, 2)$).

B. COMSIC Receiver

Fig. 1 shows the block diagram of the experimental COMSIC receiver. Two-branch antenna diversity reception was used at the BS receiver. The frequency-down converted IF signal was linearly amplified by an AGC amplifier with the dynamic range of approximately 70 dB. Then, the received spread signal at each antenna was converted into baseband I and Q components by a quadrature detector. The I and Q signals were sampled at the rate of 4×1.024 MHz (where $N_{\text{os}} = 4$ is the over-sampling factor) using 8-bit A/D converters in order to alleviate the required attenuation performance of analog-type anti-aliasing filters and were filtered by a square-root raised cosine Nyquist filter. Then, the filtered chip sequences are fed into COMSIC. The output data sequence at the COMSIC is de-interleaved and soft-decision Viterbi decoded so at to recover the transmitted data sequence. The operation of fast TPC is to be explained in Section II-C.

The block diagrams of the COMSIC and channel estimation and interference replica generation units (CEIGUs) are shown in Figs. 2 and 3, respectively. At each stage in the COMSIC, there are K CEIGUs [11]. In the CEIGU, despreading achieved through the code-synchronized correlators, respreading, and subtracting operations are implemented by a field programmable gate array (FPGA), since these operations are performed at a high rate, i.e., chip rate. The channel estimation, coherent Rake combining, i.e., the multiplication of the complex conjugate of the estimated channel gain to the despread signal of coded data symbols, tentative data decision, multiplication to the tentative decision data symbols by the estimated channel gain, and reverse-modulating are implemented by a digital signal processor (DSP). This is because that DSP is suitable for adaptive processing required for these operations, in addition that these operations are computed with the lower rate operation based on the symbol rate.

The composite signal sample sequence received on each antenna was despread using MFs. After despreading, the received signal powers of all simultaneous active users were measured using both pilot and channel-coded data symbols within a slot. In this case, resolved paths having a higher received power above a prescribed threshold were first selected (a threshold value identical to that of the path search for Rake combining was employed as explained later), and the received signal power was the summation of the selected paths in squared form. Then, the active users were ranked according to the received signal powers at each slot. The ranking operation was implemented

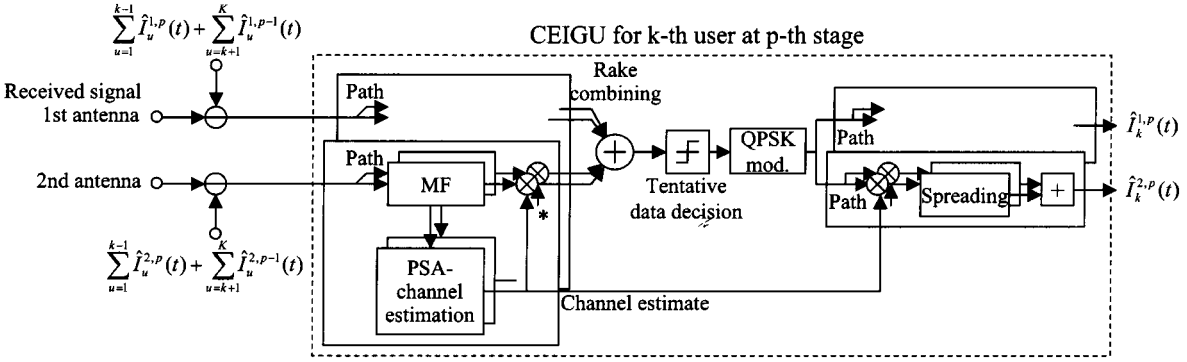

Fig. 3. CEIGU structure.

by the DSP based on a sorting algorithm and it was updated at every slot since ranking tracked the instantaneous fading variations. In each CEIGU, channel estimation, data-decision, and replica generation of the MAI are performed for each user in the order of decreasing power.

Let $I_{k,l}^{(b,p)}(t)$ be the generated replica, at the pth stage, of the kth user spread signal which is associated with the lth path received at the bth diversity antenna branch. At each stage, the MAI from $K-1$ users is subtracted from received composite signal $r^{(b)}(t)$. Expression $\hat{I}_u^{(b,p)}(t)=\sum_{l=1}^{Lu}\hat{I}_{u,l}^{(b,p)}(t)$ represents the MAI from a higher ranked user $(1 \le u \le (k-1))$ and $\hat{I}_u^{(b,p-1)}(t) = \sum_{l=1}^{Lu}\hat{I}_{u,l}^{(b,p-1)}(t)$ represents the MAI from a lower ranked users $((k+1) \le u \le K)$. The way $I_{k,l}^{(b,p)}(t)$ is generated is explained hereafter. Let $r_{k,l}^{(b,p)}(t)$ be the MF input after subtraction of MAI from $K-1$ interfering users. The MF output of the CEIGU for the lth path and the kth user in the pth stage, the despread signal $\beta_{k,l}^{(b,p)}(m,n)$ at time $t=(m+1)T+\hat{\tau}_{k,l}+nT_{\text{slot}}$, which corresponds to the mth symbol in the nth slot $(m=0,1,\ldots,N_p+N_{s-1}; n=\ldots-1,0,1,\ldots)$, is represented as

$$\beta_{k,l}^{(b,p)}(m,n)=\int_{mT+\hat{\tau}_{k,l}+nT_{\text{slot}}}^{(m+1)T+\hat{\tau}_{k,l}+nT_{\text{slot}}} r_{k,l}^{(b,p)}(t)c_k(t-\hat{\tau}_{k,l})\,dt \tag{2}$$

where $\hat{\tau}_{k,l}$ is the estimated time delay of the lth path and $T_{\text{slot}}=(N_p+N_s)T$. Using received pilot symbols $[\beta_{k,l}^{(b,p)}(m,n)]_{m=0}^{N_p-1}$, the time varying complex channel gain is estimated for coherent Rake combining followed by a tentative data decision.

In an actual propagation channel such as that in vehicular environments, the received power of each path dynamically varies along with the time delay. Therefore, we must select and update the paths having a sufficient signal-to-interference ratio (SIR), which effectively contribute to Rake combining. Furthermore, the number of effective paths naturally changes. Conventional code tracking methods such as delay locked-loop (DLL) or tau dither loop (TDL) have a robust feature for tracking one specified path with a time-invariant power. However, these tracking methods cannot track the frequency updating of an effectual path for Rake combining. Therefore, in the paper, the search of the propagation paths, i.e., the estimation of the time delay of each path required for Rake combining, is conducted using the block-average power delay profile as follows (see Fig. 4).

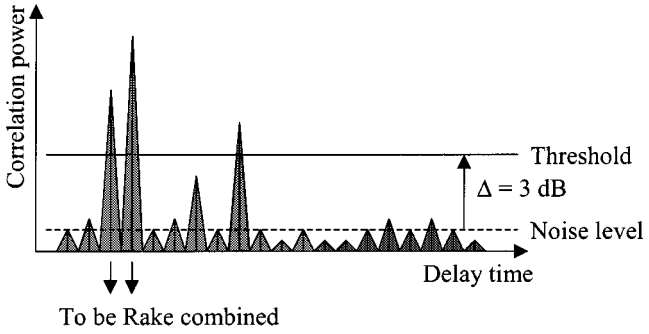

Fig. 4. Path search procedure.

First, the instantaneous power delay profile is measured by coherently adding the despread signals of N_p pilot symbols belonging to each slot. Let $\bar{\Lambda}^{(n)}(\tau)$ be the measured instantaneous power delay profile at nth slot. Then, using a first-order filter, the average power delay profile is further measured by $\hat{\Lambda}^{(n)}(\tau)=\mu\hat{\Lambda}^{(n-1)}(\tau)+(1-\mu)\bar{\Lambda}^{(n)}(\tau)$, where μ is the forgetting factor. That is, as the value of μ approaches 1, the equivalent averaging interval becomes longer. In the receiver, we used $\mu=0.99375$, this corresponds to averaging over 10 frames (=100 ms interval). While the instantaneous phase and amplitude vary within one slot due to fading, the average power delay profile shape can be assumed to remain unchanged over a 100-ms interval. From the laboratory and field experiments, the 100-ms measurement interval was found to minimize the average bit error rate (BER) after Rake combining. The time delay resolution for the power delay profile measurement was 1/4-chip (=244.1 ns =73.2 meters). Paths having a received power above a predetermined threshold, which was set to 3-dB greater than the average power except for the power of four paths from the largest in the measured power delay profile, were recorded and the strongest $\hat{L}_u$ paths were selected for Rake combining $(1 \le \hat{L}_u \le 4)$. When the number of paths exceeded four, the sources of MAI from the excessive paths beyond four nevertheless having the lower average received power were not removed. However, we already elucidated that the number of dominant paths having an efficient SIR for Rake combining is less than four based on the field experiments conducted near Tokyo [19]. Thus, it is considered that the impact of the residual MAI from the excessive paths beyond the number of Rake fingers is small.

The tentative decision rule on $\phi_k^{(p)}(m,n)$ is represented as

$$\hat{\phi}_k^{(p)}(m,n) = \max_{\phi\in(n\pi/2;n=0,\ldots,3)} \mathrm{Re}\left\{\left(\sum_{b=1}^{2}\sum_{l=1}^{\hat{L}u}\beta_{k,l}^{(b,p)}(m,n) \times \hat{\xi}_{k,l}^{(b,p)*}(m,n)\right) \exp(-j\phi+\pi/4)\right\} \quad (3)$$

where $\hat{\xi}_{k,l}^{(b,p)}(m,n)$ is the estimated channel gain of $\xi_{k,l}^{(b)}(m,n)$ and $\mathrm{Re}[\cdot]$ and * denote the real part and the complex conjugate, respectively. The channel estimate, $\xi_{k,l}^{(b,p)}(m,n)$, of the kth user associated with the lth path of the nth slot for the bth antenna branch at the pth stage was obtained by coherently averaging the despread signal of N_p pilot symbols belonging to two successive slots as [17] and [18]

$$\hat{\xi}_{k,l}^{(b,p)}(m,n) = \frac{\sum_{m=0}^{Np-1}\left[\beta_{k,l}^{(b,p)}(m,n)+\beta_{k,l}^{(b,p)}(m,n+1)\right]}{2N_p}. \quad (4)$$

Using $\hat{\phi}_k^{(p)}(m,n)$ and $\hat{\xi}_{k,l}^{(b,p)}(m,n)$ the replica of MAI over the time interval of the nth slot is regenerated as

$$\hat{I}_{k,l}^{(b,p)}(t) = \hat{\xi}_{k,l}^{(b,p)}(t)\hat{d}_k^{(p)}(t)c_k(t). \quad (5)$$

where $\hat{d}_k^{(p)}(t) = \sum_{m=nT_{\mathrm{slot}}}^{N_p+N_s+nT_{\mathrm{slot}}-1}[\exp(j\hat{\phi}_k^{(p)}(m))]u(t/T-m)$. Using the MAI replica, MF input for the lth path of the bth antenna at the pth stage is generated as

$$r_{k,l}^{(b,1)}(t) = r(t) - \sum_{i=1}^{k-1}\sum_{j=1}^{\hat{L}u}\hat{I}_{i,j}^{(b,1)}(t-\hat{\tau}_{i,j}) \quad \text{for } p=1, \quad (6)$$

$$r_{k,l}^{(b,p)}(t) = r(t) - \left[\sum_{i=1}^{k-1}\sum_{j=1}^{\hat{L}u}\hat{I}_{i,j}^{(b,p)}(t-\hat{\tau}_{i,j}) + \sum_{i=k+1}^{K}\sum_{j=1}^{\hat{L}u}\hat{I}_{i,j}^{(b,p-1)}(t-\hat{\tau}_{i,j})\right] \quad \text{for } p\geq 2. \quad (7)$$

Since the MAI subtraction and channel estimation operation are performed for each user in the order of decreasing received powers, the accuracy of the channel estimation for lower ranked users improves. Furthermore, this successive channel estimation for different users is repeated in each canceling stage and thus, the accuracy of the channel estimation for the same user improves at a higher canceling stage.

Expression $[\hat{\phi}_k^{(p)}(m,n)]_{k=0}^{K-1}$ give the recovered mth QPSK symbols of K users at the last stage $p=P$. The maximum number of stages of the experimental receiver was three, i.e., $P=3$. The last stage output of user k is given by $\hat{\eta}_k(m,n)=\sum_b\sum_l\beta_{k,l}^{(b,P)}(m,n)\hat{\xi}_{k,l}^{(b,P)*}(m,n)$. The sequence of $\mathrm{Re}[\hat{\eta}_k(m,n)]$, $\mathrm{Im}[\hat{\eta}_k(m,n)]$ is the soft-decision data sequence corresponding to transmitted coded binary data and is deinterleaved and soft-decision Viterbi decoded to recover the transmitted data of user k. In the implemented COMSIC receiver, the sampled data sequences with four times the chip rate of the baseband I/Q signals over the duration of one frame interval, i.e., 16-slot interval, are restored in the memory. The delay time for one-stage processing of multistage interference canceling is two-slot per user (i.e., one-slot interval is consumed by despreading, coherent channel estimation, Rake combining, and tentative data decision, and another one-slot interval is for multiplication of the estimated channel gain and respreading). This processing delay time is proportional to the number of simultaneous active users up to K $(=SF)$. However, the processing time delay can be decreased by using a much faster clock rate. The inherent time delay is due to the interleaving in the time domain for channel coding and decoding and this is identical to the MF-based Rake receiver.

We compared the processing complexity of COMSIC to that of the MF-based Rake receiver based on the number of operations of complex-valued multiplications (hereafter simply multiplications). The number of multiplications needed for each constituent process of COMSIC and that of the MF-based Rake receiver is listed in Table II. In each stage except for the final stage, operations such as inverse-modulation required for decision-feedback channel estimation, multiplication of the estimated channel gain by the decision data symbols, multiplication of the interference rejection weight, and respreading to regenerate the MAI replica are added to the operations needed for the MF-based Rake receiver. Meanwhile, the process of the final stage is identical to that of the MF-based Rake receiver. Then, based on the number of multiplications listed in Table II, we calculated the total number of multiplications per slot of COMSIC with the number of stages as a parameter and that of the MF-based Rake receiver in Table III. In Table III, we assumed that $N_s=N_p+N_d=40$ symbols, $SF=16, K=16$ codes, and $L=2$ paths. The ratio of the relative complexity with that of the MF-based Rake receiver as a reference is also shown in parentheses. Table III indicates that the complexity of the three-stage COMSIC is almost five times that of the MF-based Rake receiver.

C. SIR Based Fast TPC Suitable for COMSIC

SIR-based closed-loop TPC [21] was used as the fast TPC. The relationship between the required MS transmission power and the TPC delay was clarified in [19]. To restrict the increase of the required MS transmission power within 0.5 dB, the TPC delay must be within an interval of several slots. In general, COMSIC accompanies the processing delay beyond an interval of several slots especially when the number of active users, K, is large. Even for the parallel-type COMSIC, in which channel estimation, data decision, and MPI replica generation are performed simultaneously at the same stage, a long processing delay proportional to the number of stages is required. Thus, it is almost impossible to realize TPC with a several-slot duration delay when we measure the SIR after interference canceling at the COMSIC output as shown in Fig. 5(a). Therefore, we propose a SIR measurement based fast TPC method suitable for COMSIC as shown in Fig. 5(b). In the proposed method, the SIR after Rake combining is measured at the MF-based Rake combiner output, i.e., before MAI suppression, not at

TABLE II
NUMBER OF MULTIPLICATIONS IN COMSIC

	MF based Rake receiver	COMSIC	
		p-th stage	Final stage
Despreading	$K \times N_s \times N_{os} \times SF \times L$	$K \times N_s \times N_{os} \times SF \times L$	$K \times N_s \times N_{os} \times SF \times L$
Channel compensation	$K \times N_s \times L$	$K \times N_s \times L$	$K \times N_s \times L$
Inverse-modulation		$K \times N_s \times L$	
Multiplication of channel		$K \times N_s \times L$	
Re-spreading		$K \times N_s \times N_{os} \times SF \times L$	
Total	$K \times N_s \times L \times (N_{os} \times SF + 1)$	$K \times N_s \times L \times (2N_{os} \times SF + 3)$	$K \times N_s \times L \times (N_{os} \times SF + 1)$

TABLE III
COMPLEXITY COMPARISONS BETWEEN COMSIC AND MF-BASED RAKE RECEIVER

		Multiplication	Example (Ratio to MF w/o COMSIC) when $K = 16$, $N_s = 40$, $N_{os} = 4$, $SF = 16$, $L = 2$
MF based Rake receiver		$K \times N_s \times L \times (N_{os} \times SF + 1)$	8.32×10^4 (1.00)
COMSIC	2 stages	$K \times N_s \times L \times (3N_{os} \times SF + 4)$	2.51×10^5 (3.02)
	3 stages	$K \times N_s \times L \times (5N_{os} \times SF + 7)$	4.19×10^5 (5.04)
	4 stages	$K \times N_s \times L \times (7N_{os} \times SF + 10)$	5.86×10^5 (7.04)

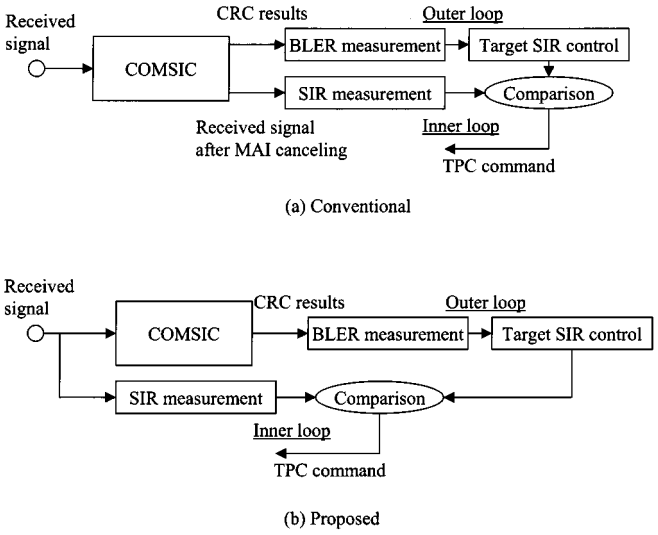

Fig. 5. COMSIC with outer loop TPC . (a) Conventional. (b) Proposed.

the COMSIC output. However, the target SIR value of the MF-based Rake combiner output for satisfying the required quality such as the block error rate (BLER) or BER is different from that of the COMSIC output since the MAI is sufficiently suppressed at the COMSIC output. Therefore, the target SIR value for SIR measurement at the MF-based Rake combiner output is compensated by the outer loop control so that the measured BLER value at the COMSIC output is equal to the prescribed target value. Since the SIR measurement is conducted in the same way an in the MF-based Rake receiver, fast TPC within a delay of several slots is achieved.

The operation of fast TPC used in the paper is described hereafter. In this paper, instead of measuring the SIR after Rake combining, we apply the SIR measurement method proposed in [22], in which, first, the SIR on each resolved path is measured and then, the SIRs of all the resolved paths are summed to obtain the SIR (which is equivalent to the one at the output of the Rake combiner). By doing so, an SIR measurement that has less influence on the channel estimation error is possible. Therefore, we measured the SIR associated with each resolved path and then summed them to obtain the SIR that corresponds to the SIR after Rake combining. The SIR measurement is summarized below. First, signal power $\tilde{S}_l(n)$ of the nth slot associated with the lth path is computed using the received ten symbols including $N_p = 4$ pilot symbols. Signal power $\tilde{S}_l^{(b)}(n)$ of lth path at bth antenna is given by

$$\tilde{S}_l^{(b)}(n) = |\bar{\beta}_l^{(b)}(n)|^2 \tag{8}$$

where

$$\bar{\beta}_l^{(b)}(n) = \frac{1}{10}\left[\sum_{m=1}^{4} \beta_l^{(b),\mathrm{MF}}(m,n)\exp\left(-\frac{j\pi}{4}\right) + \sum_{m=5}^{10} \beta_l^{(b),\mathrm{MF}}(m,n)\exp(-j\tilde{\phi}^{\mathrm{MF}}(m,n))\right] \tag{9}$$

and $\beta_l^{(b),\mathrm{MF}}(m,n)$ is the resolved path component received at the bth antenna, $\tilde{\phi}^{\mathrm{MF}}(m,n)$ is the tentative decision in the MF-based Rake receiver on the mth symbol of the nth slot. The first term in the square brackets is the contribution from N_p pilot symbols with the modulation phase of $\pi/4$ radians. Term $\tilde{\phi}^{\mathrm{MF}}(m,n)$ is obtained in the same way as in (3) for the data symbols with $m = 5$–10, nevertheless, it becomes $\pi/4$ radius for pilot symbols with $m = 1$–4. The instantaneous interference plus background noise power of the lth path at bth

antenna, $\tilde{I}_l(k)$, is computed as the squared error of the received four pilot samples and six data samples

$$\tilde{I}_l^{(b)}(n) = \frac{1}{10}\sum_{m=1}^{10}\left|\beta_l^{(b),\mathrm{MF}}(m,n)\exp(-j\tilde{\phi}^{\mathrm{MF}}(m,n)) - \bar{\beta}_l^{(b)}(n)\right|^2. \tag{10}$$

Then, $\tilde{I}_l^{(b)}(n)$ is averaged using a first-order filter with forgetting factor $\gamma(<1)$ to obtain

$$\bar{I}_l^{(b)}(n) = \gamma\bar{I}_l^{(b)}(n-1) + (1-\gamma)\tilde{I}_l^{(b)}(n). \tag{11}$$

The SIR at the nth slot associated with the lth path at bth antenna $\tilde{\lambda}_l^{(b)}(n)$ is given by

$$\tilde{\lambda}_l^{(b)}(n) = \tilde{S}_l^{(b)}(n)/\bar{I}_l^{(b)}(n) \tag{12}$$

and finally, the SIR at the nth slot, $\bar{\lambda}(n)$, is obtained as

$$\bar{\lambda}(n) = \sum_{b=1}^{2}\sum_{l=0}^{Lk-1}\tilde{\lambda}_l^{(b)}(n). \tag{13}$$

In the experiment, $\gamma = 0.993\,75$ was used (i.e., the SIR measurement interval becomes $1/(1-\gamma) = 160$ slots $= 100$ ms) so that fast variation due to fading can be sufficiently averaged, while shadowing remains unchanged. In the following section, we used the signal energy per bit-to-interference plus background noise spectrum density ratio (E_b/I_0) instead of $\bar{\lambda}(n)$. The E_b/I_0 can be expressed using $\bar{\lambda}(n)$ as $E_b/I_0(n) = \bar{\lambda}(n) + 10\log(3/2)$ dB since rate-$1/3$ convolutional coding and QPSK data modulation were used. Then, the MS controls the transmission power with a step size of Δ_{in} dB slot-by-slot according to the TPC bit sent from the BS so that the measured E_b/I_0 is equal to the target value.

In our outer loop control scheme, the target E_b/I_0 is controlled based on the BLER measurement results after soft-decision Viterbi decoding. More concretely, the target E_b/I_0 is compensated as follows, where M_{ERR} is the number of block errors within the number of total measured blocks, H:

- When $M_{\mathrm{ERR}} > M_{\mathrm{UPP}}$, the target E_b/I_0 is increased by Δ_{OUT}.
- When $M_{\mathrm{ERR}} < M_{\mathrm{LOW}}$, the target E_b/I_0 is decreased by Δ_{OUT}.
- When $M_{\mathrm{LOW}} \leqq M_{\mathrm{ERR}} \leqq M_{\mathrm{UPP}}$, the target E_b/I_0 is not compensated;

where M_{UPP} and M_{LOW} are the upper and lower block-error thresholds, respectively, and identical values were used, i.e., $M_{\mathrm{LOW}} = M_{\mathrm{UPP}} = M$. Thus, the target E_b/I_0 value is a constant value within each updating interval, i.e., H-block duration. Another outer loop control scheme based on the instantaneous block error of every block was proposed in [22]. In that method, when block error is detected, the target E_b/I_0 value is increased by Δ_{inc} and when all coded-data bites within the block are decoded without errors, it is decreased by Δ_{dec}, using the asymmetric step size of Δ_{inc} and Δ_{dec}. However, it was reported in [22] that although the BLER over the short term using the method based on the instantaneous block errors can approach the target BLER rather than that based on the BLER over H-blocks, the improvement is slight. Thus, we used the former method in the experiments.

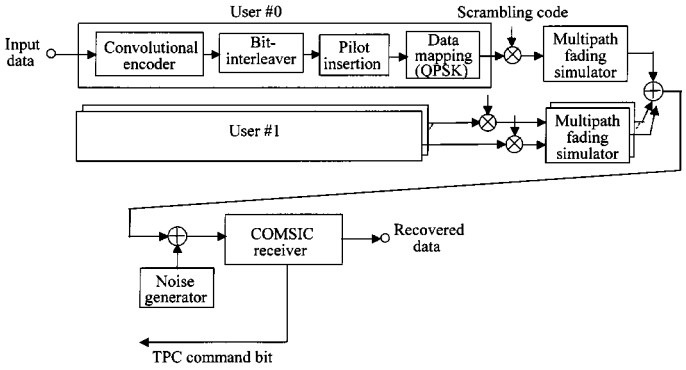

Fig. 6. Experiment configuration.

III. Experimental Results

The configuration of the experimental system is illustrated in Fig. 6. The transmitted spreading signals of MSs are fed into an independent multipath fading simulator. In the experiments, we employed hardware multipath fading simulators using the same carrier frequency interface as that of the implemented transceiver in a 2-GHz bandwidth. The shape of the delay profile and the time delay of each path are generated independently from the reference clock timing in the COMSIC receiver. The transmitted spreading signals of the MSs are fed into an independent multipath fading simulator. Fading simulators generate multipath signals that follow independent L-path Rayleigh fading with average equal power and with the maximum Doppler frequency, f_D. The time delay difference between paths was set to 1.0 μs corresponding to a chip length of 1.0. After suffering independent L-path Rayleigh fading of f_D with equal average received power and added Gaussian noise, the composite signal is received at the COMSIC receiver at the BS. The received timing of the spreading signal from the MSs was asynchronous within one data symbol duration. The time delay and channel gain associated with each path of all active users were independently estimated in the experimental results presented in Sections II-B and II-C irrespective of the channel model. In the experiment with fast TPC, the TPC delay in the inner loop was two slot lengths and the received signal power at each MS in the forward link was set to be sufficiently high so that no TPC command bit error occurred. Assuming identical received quality, e.g., BLER or BER, the transmission power is proportional to the symbol rate. Thus, in mixed traffic situations, the achievable received quality of low-rate users is more degraded compared with that of high-rate users since the low-rate users suffer from severe MAI. Then, the COMSIC is more effective for low-rates users than for high-rate users. Therefore, the aim of this paper is to elucidate clearly the BER improvement of low-rate users experiencing severe MAI from high-rate users who transmit at high power. We measure the BER performance of the low rate desired user, i.e., $k = 1$ to indicate the aforementioned effect.

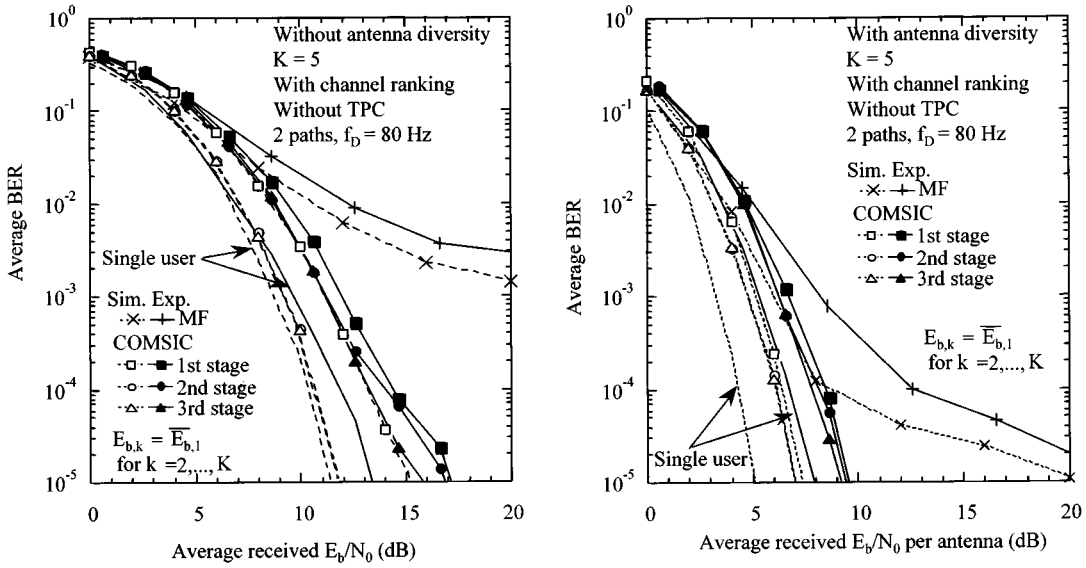

Fig. 7. Average BER performance with the number of stages as a parameter. (a) Without antenna diversity. (b) With antenna diversity.

A. BER Performance Without Fast TPC

We first investigate the interference suppression effect of COMSIC independently from the influence of fast TPC. We measured the BER performance of the desired user under the conditions in which there was no fading channel, i.e., AWGN channels were assumed for the other interfering users due to the restriction of hardware fading simulators from Figs. 7–12. However, we confirm the validity of this assumption in the evaluations of Figs. 13 and 14. The effect of the number of canceling stages on the average BER performance is plotted in Fig. 7 as a function of average signal energy per information bit-to-background noise spectrum density ratio (E_b/N_0) when $K = 5$ (the link load normalized by SF corresponds 21%) without [Fig. 7(a)] and with antenna diversity reception [Fig. 7(b)]. The results of the MF-based Rake receiver are also plotted for comparison. The BER measurement was performed on user $k = 1$ only. The other users were considered as interfering users. In this measurement, other user signals that were not faded were received with the powers equal to the average power of user $k = 1(E_{b,k}/N_0 = \bar{E}_{b,1}/N_0, k = 2, \ldots, K)$. The value of f_D, was 80 Hz which corresponds to a mobile speed of 43.4 km/h at the carrier frequency of 1.9905 GHz. The computer simulation results are also plotted for comparison. There are two main differences between the computer simulation results and the experimental results. First, in the simulation results, the amplitudes of transmitted and received signals were not quantized because an almost infinite dynamic range of amplitude is assured. Meanwhile, the band-limited data sequence in the baseband I/Q channels were quantized by 8-bit D/A converters in the transmitter and the baseband analog I/Q channels were quantized by 8-bit A/D converters associated with the linear AGC amplifier with a dynamic range above 70 dB. The second is the assumption of the ideal estimation of the time delay of each path; therefore, no band limitation is applied in the simulations. However, the time delay of each resolved path was actually estimated for the over-sampled data sequence with four times the chip rate in the experimental receiver.

Figs. 7(a) and (b) shows that the BER performance improves as the number of canceling stages, p, increases; however, additional improvement in the performance is small when p is increased from two to three. Therefore, the use of three-stages $(P = 3)$ seems to be sufficient. In the case of the MF-based Rake receiver, an error floor is observed. However, using the three-stage COMSIC receiver, the average BER continuously decreases as the average E_b/N_0 increases; the E_b/N_0 loss from the single-user case with antenna diversity (without antenna diversity) is approximately 1.0 (1.5) dB, respectively, when $K = 5$. The degradation of the experimental results from the simulation results at the first, second, and third stages are 1.5 (1.0), 1.5(2.0), and 1.5 (2.0) dB with (without) antenna diversity reception, respectively. This degradation is considered to be caused by the path search error for Rake combining and quantization by A/D converters. In the following experiments, we measured the BER performance of the three-stages.

The measured average BER performance with COMSIC is plotted with the simultaneous active users, K, as a parameter and as a function of the average received E_b/N_0 in Fig. 8 for no antenna diversity [Fig. 8(a)] and antenna diversity [Fig. 8(b)]. A nonfading channel and equal received signal power as the average power of the $k = 1$ user were also assumed for the users $k = 2, \ldots, K(E_{b,k}/N_0 = \bar{E}_{b,1}/N_0)$. The figures show that the BER performance of the COMSIC significantly improves compared with that of the MF-based Rake receiver especially for the antenna diversity reception case. When K is greater than 13, although the error floor occurs and the BER degrades above 10^{-2} for the MF-based Rake receiver, no error floor above 10^{-4} is observed for the COMSIC for the antenna diversity case. Even when $K = 16$, which corresponds to the normalized spreading factor, K/SF, of 100% and normalized processing gain K/P_g of 66.7%, the average BER below 10^{-3} can be achieved at the

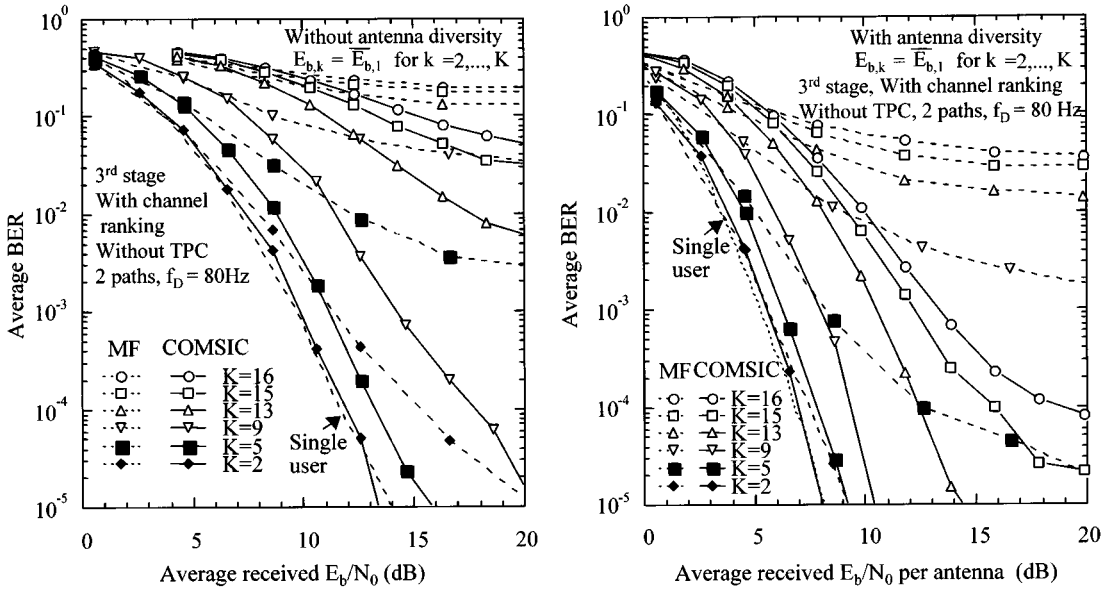

Fig. 8. Average BER performance with the number of active users as a parameter. (a) Without antenna diversity. (b) With antenna diversity.

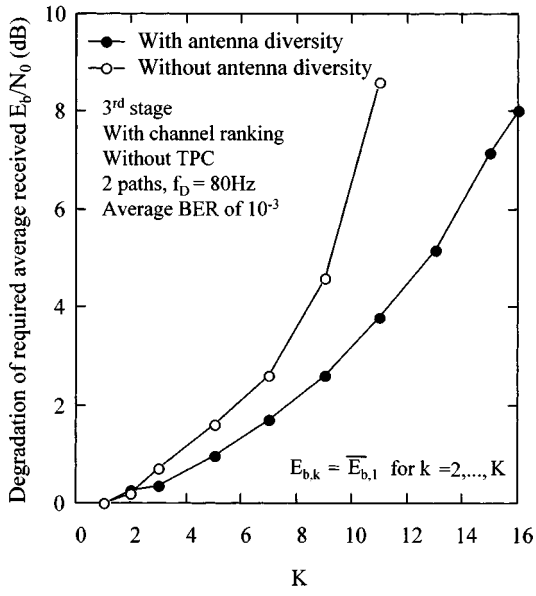

Fig. 9. Average received E_b/N_0 degradation from single-user case (noise enhancement).

average received E_b/N_0 per antenna of approximately 14 dB with antenna diversity reception.

Fig. 9 shows the loss of the required received E_b/N_0 at the average BER of 10^{-3} from that of the single user, which is referred to as noise enhancement. Experimental conditions were the same as in Fig. 8. As K is increased, the loss of the required received E_b/N_0 from the single-user case increases due to the residual MAI. When $K = 9$ or 16, however, the loss of the required received E_b/N_0 at the average BER of 10^{-3} from the single-user case is approximately 2.2 dB or 8 dB, respectively, for the antenna diversity case.

Until now, the received signal power of the interfering users has been assumed to be equal to the average power of the desired user. Thus, we investigate the BER performance when the received signal power of the interfering users is much higher than that of the average power of the desired user, which corresponds to an environment such that high-rate interfering users exist. The validity of this approximated model is explained as follows. An MAI replica is generated using the estimated channel gain, tentative decision data, and estimated time delay of each path for respreading. Among these three factors, the approximation such that increasing the transmission power with the same symbol rate has the same effect as high-rate transmission on the estimation of the channel gain and the time delay of each path. This is because the estimation accuracy of the channel gain and the time delay of each path are determined by the total received power of the pilot symbols within a slot (note that the channel gain and time delay were estimated using only pilot symbols). Therefore, this approximation only influences the tentative data decision results since the SF is different in these two situations. However, we elucidated by computer simulation that in the generation of the MAI replica, the influence of the channel gain estimation is most dominant [11], [13]. It is understood that even when the BER after Rake combining is near 10^{-1} (note that when the required BER after channel decoding is 10^{-3}, the BER after Rake combining approaches 10^{-1}), the impact of the data decision error on the MAI replica generation occurs once every ten symbols. Therefore, we can equivalently regard the increase in the transmission power of interfering users with the identical symbol rate as high-rate interfering users.

Figs. 10 and 11 plot the BER performance when the received $E_{b,k}/N_0$ of the nonfaded interfering user $(k = 2, \ldots, K)$ was greater than $\bar{E}_{b,1}/N_0$ by 3 dB and 5 dB, respectively. Figs. 10(a) and 11(a), and 10(b) and 11(b) show the BER performance without and with two-branch antenna diversity reception, respectively. The BER performance when the received powers of the interfering users are 3 dB greater than the average power of the desired user is almost the same in the case of $E_{b,k}/N_0 = \bar{E}_{b,1}/N_0$ by using the COMSIC (compare

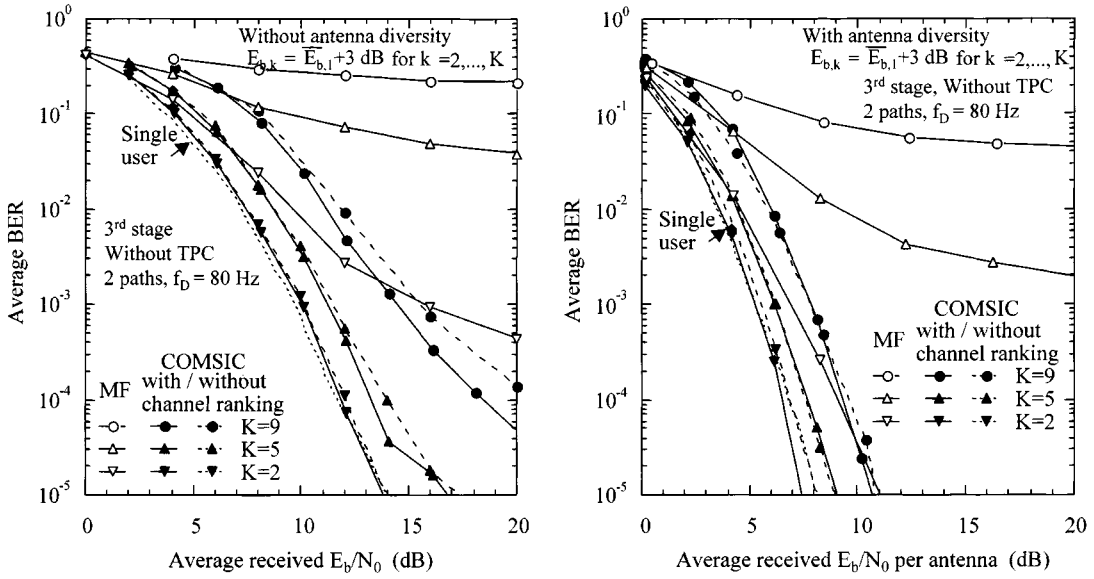

Fig. 10. Average BER performance when high transmission power users exist. (a) Without antenna diversity. (b) With antenna diversity.

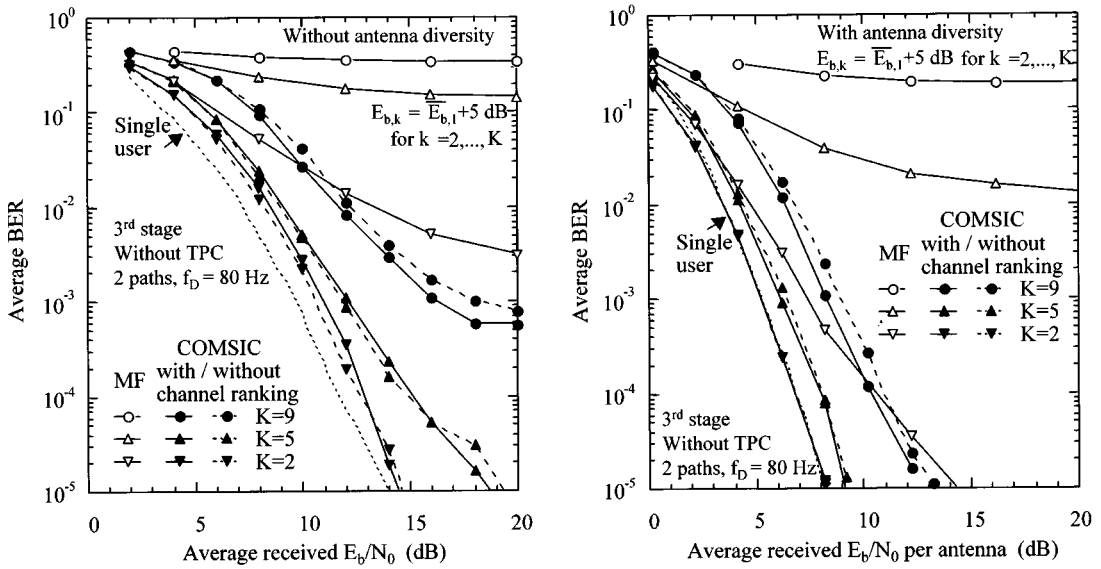

Fig. 11. Average BER performance when high transmission power users exist. (a) Without antenna diversity. (b) With antenna diversity.

Figs. 10(a) and (b), and Figs. 8(a) and (b). On the other hand, when $E_{b,k}/N_0 = \bar{E}_{b,1}/N_0 s + 3$ dB, the BER performance of the MF receiver heavily degrades due to the increased MAI. From Fig. 11, even when $E_{b,k}/N_0 = \bar{E}_{b,1}/N_0 + 5$ dB, almost the same BER performance as the case of $E_{b,k}/N_0 = \bar{E}_{b,1}/N_0$ is observed by using the COMSIC with antenna diversity reception (the loss of the required received E_b/N_0 at the average BER of 10^{-3} is within 0.5 dB when $K = 9$). When antenna diversity reception is not applied, the BER performance for $E_{b,k}/N_0 = \bar{E}_{b,1} + 5$ dB is slightly degraded compared with that for $E_{b,k}N_0 = \bar{E}_{b,1}/N_0$ due to the error of the regenerated interference replica (the loss of the required received E_b/N_0 at the average BER of 10^{-3} is approximately 1.5 dB when $K = 9$). On the other hand, an error floor is observed at a low BER for the MF-based Rake receiver. We clarified that the COMSIC is effective in reducing the interference from the high transmission power users (high bit rate users).

The BER performance without channel ranking according to the received signal level is also shown in Figs. 10 and 11. In this case, it was assumed that the channel estimation using pilot symbols, coherent Rake combining, and tentative data decision of the desired user was first performed at each stage. Thus, since the channel estimation must be performed in a very low SIR channel where the received signal power of all interfering users are 3 or 5 dB higher than that of the desired user, it is expected that the BER performance degrades compared with the case with channel ranking due to the error of the regenerated interference replica. From the figures, when the number of interfering users is high such as $K = 9$, although the BER performance with channel ranking improves compared with the case without

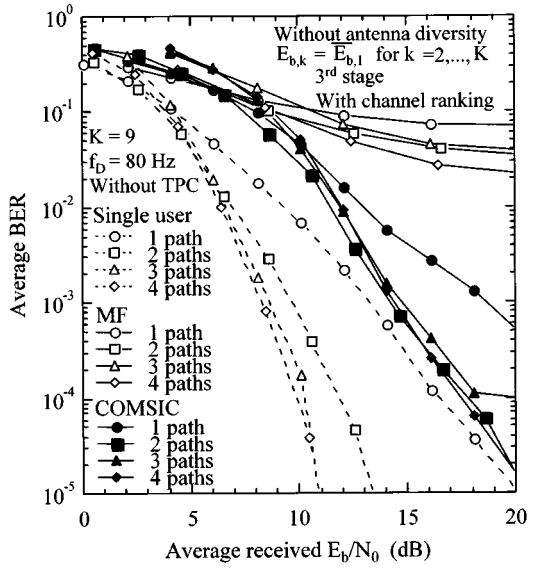

Fig. 12. Effect of the number of multipaths.

channel ranking, this improvement is small. The reason for this is considered to be that the accuracy of the power level ranking degrades as K is increased because the received signal power level per slot length of each user must be measured in a low SIR channel before interference canceling. When K is small, the effect of power level ranking is not observed since the MAI is small.

The measured average BER performance as a function of average received E_b/N_0 is plotted in Fig. 12 with the number of multipaths as a parameter. It was assumed that $E_{b,k}/N_0 = \bar{E}_{b,1}/N_0$ and $f_D = 80$ Hz. The BER performance is plotted both for the case with and without antenna diversity. The BER performance of the single-user case is also shown for comparison. For the single-user case, the BER performance improves as L is increased due to the Rake time diversity effect. However, the improvement from $L = 3$ to 4 is negligible. This is because the degradation in the channel estimation error due to the decreased signal power per path exceeds the improvement caused by the Rake time diversity effect. For the COMSIC receiver, almost the same BER performance is obtained for $L = 2$–4. The BER of COMSIC significantly improves compared with the MF-based Rake receiver because it regenerates an MAI replica for all four-paths and satisfactorily subtracts them from the received signal.

So far, the BER performance of the desired user was measured assuming no fading channel for the other interfering users. However, in Fig. 13, the BER performance of the desired user was measured assuming a two-path independent Rayleigh fading channel with equal average power for all interfering users until $K = 5$ (the number of interfering users was four). The average received signal power of each interfering user was equal to that of the desired user ($\bar{E}_{b,k}/N_0 = \bar{E}_{b,1}/N_0$). It was assumed that $f_D = 80$ Hz. Without antenna diversity, an error floor above the average BER of 10^{-3} is observed due to the MAI for the MF-based Rake receiver. However, no error floor is observed for the COMSIC receiver. The loss of the required received E_b/N_0 from the single-user case is approximately 1.5 dB and 2.0 dB at the average BER of 10^{-3} for with and without antenna diversity, respectively. It is clear from the comparison between Figs. 8 and 13 that when $K = 5$, the achievable BER performance assuming no fading channel for the interfering users is almost identical to that assuming a two-path independent Rayleigh fading channel for all the interfering users owing to the statistical multiplexing effect theoretically based on the central-limit theorem. Furthermore, this result implies that the channel estimation is satisfactorily performed for an interfering channel.

The required received E_b/N_0 for obtaining the average BER of 10^{-3} is shown in Fig. 14 as a function of f_D. In the same way as in Fig. 13, the power delay profile of two-discrete paths, which were independently subjected to Rayleigh fading, was assumed for all users. Since the fast TPC is not applied, as f_D increases, the BER performance monotonously improves due to the increased interleaving and channel coding effect. As K is increased, the BER performance degrades being shifted in parallel due to the increasing MAI. It is clearly seen from the figure that the pilot symbol-assisted channel estimation can track the fast fading, and the MAI replica is generated properly when f_D is lower than approximately 320 Hz.

B. BER Performance With Fast TPC

1) BER Performance as a Function of the Number of Active Users: We first investigated the effect of successive channel estimation by computer simulation. Fig. 15 shows the average BER performance of the three-stage COMSIC with the stage index, P_{CE}, when the channel estimation needed for generating an MAI replica is a parameter and as a function of the average transmit E_b/N_0 of the desired user, where the transmit E_b/N_0 is the transmission power per bit normalized by the background noise spectrum density. For example, when P_{CE} was the second- stage, the channel gain estimated at the second- stage was used at the third stage. It was assumed that the same frame structure as the experiment COMSIC transceiver was used and that $K = 15$, i.e., 14 interfering users with independent $L = 2$ paths Rayleigh fading channel with $f_D = 80$ Hz. Fig. 15 indicates that even with the same stages, when P_{CE} is the first stage, the BER performance of COMSIC is degraded compared with the that with $P_{\mathrm{CE}} = 3$rd stage, i.e., successive channel estimation. This is because the deteriorated channel gain due to the severe MAI estimated at the first stage is employed at the second and third stages, resulting in the degradation of the regenerated MAI replica. Although the improvement from P_{CE} =second stage to third stage is slight, the effect of successive channel estimation at each stage is validated. The subsequent results were measured by laboratory experiments using hardware fading simulators.

Next, the measured average BER performance levels with and without antenna diversity reception are plotted in Figs. 16 and 17, respectively, with the value of K as a parameter. The average BER performance without an outer loop is shown as a function of the target E_b/I_0 per antenna of fast TPC and average transmission power of a MS in Figs. 16(a) and 17(a), and 16(b) and 17(b), respectively. The MS transmission power was normalized by that for achieving the average BER of 10^{-3} using the COMSIC receiver when $K = 2$ and $f_D = 80$ Hz. It

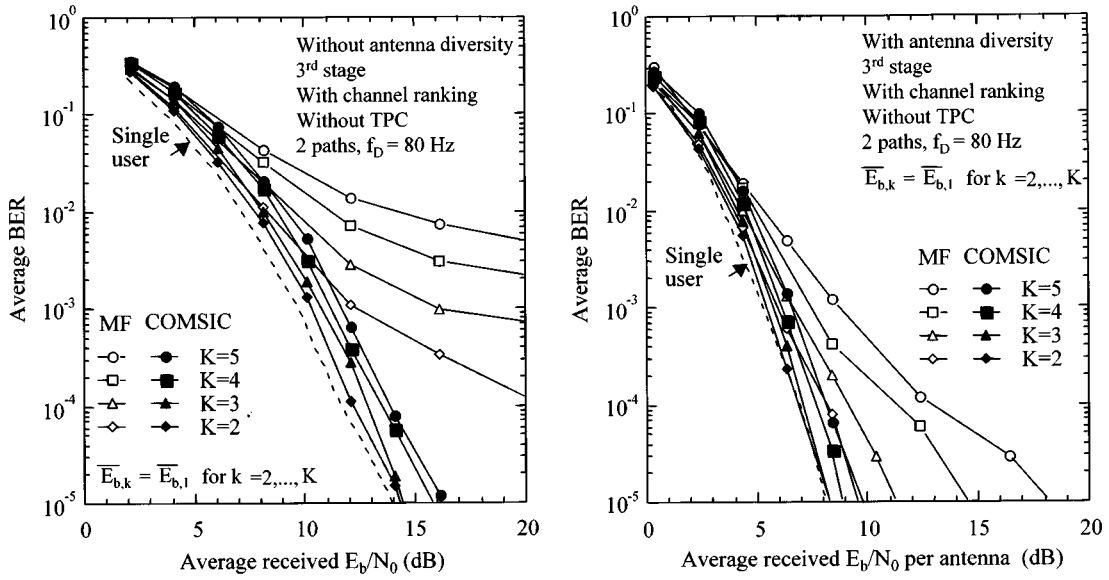

Fig. 13. Average BER performance with the number of active users as a parameter. (a) Without antenna diversity. (b) With antenna diversity.

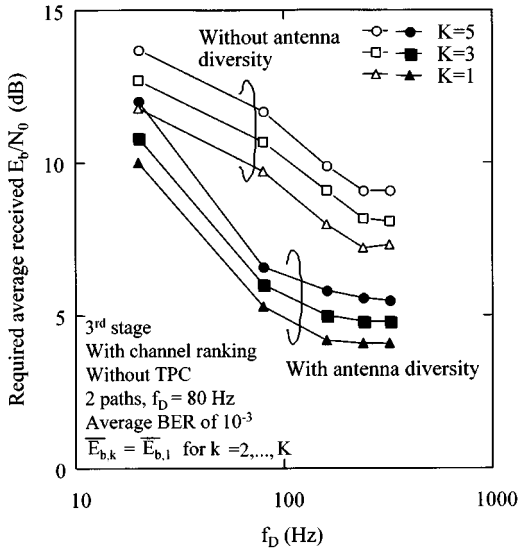

Fig. 14. Required average received E_b/N_0 performance as a function of f_D.

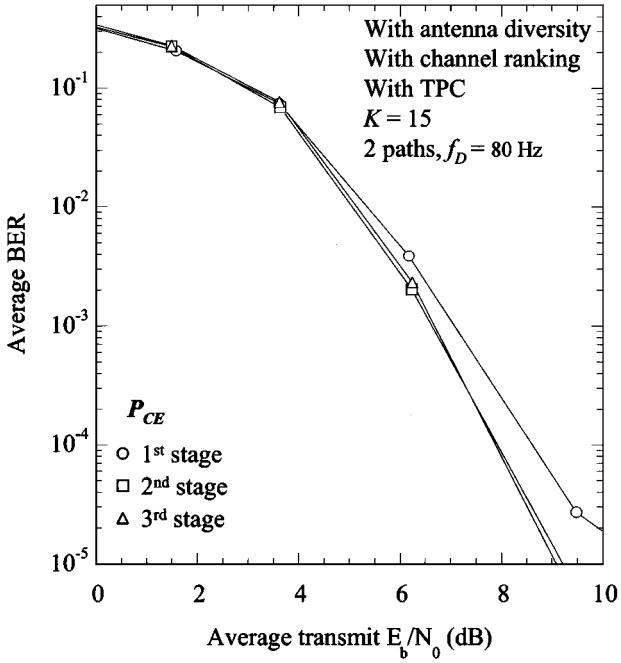

Fig. 15. Effect of successive channel estimation.

was assumed that $L = 2$ and $f_D = 80$ Hz. The performance with the MF-based Rake receiver is also shown for comparison. Figs. 16(a) and 17(a) show that almost the same BER performance is achieved with the MF-based Rake receiver irrespective of K, that is the aggregated interference, since the target E_b/I_0 is identical. Meanwhile, the average BER performance with COMSIC is improved as K is increased because the interference that is suppressed is increased. In other words, although the MAI from one interfering user is suppressed for $K = 2$, the MAI from seven interfering users is cancelled for $K = 8$. This brings about a significant increase in the SIR at the COMSIC output. On the other hand, from Figs. 16(b) and 17(b), the required MS transmission power of the MF-based Rake receiver is evidently increased as K, i.e., MAI, is increased so as to satisfy the target E_b/I_0 value. When $K = 6$, the required target E_b/I_0 with COMSIC for the average BER of 10^{-3} could be decreased by approximately 1.0 dB compared with the MF-based Rake receiver. At the same time, the required MS transmission power could be decreased by approximately 3.0 dB.

Comparing Figs. 16 and 17, when K is large, the improvement in the achieved BER performance with antenna diversity reception using COMSIC is decreased compared with the case without antenna diversity. This is because the accuracy of the generated MAI replica is degraded mainly due to the increased channel estimation error caused by the decreased signal power per path. With antenna diversity reception, the required average MS transmission power (target E_b/I_0) with COMSIC for satisfying the average BER of 10^{-3} is decreased by approximately 2.0 (0.5) dB compared with the MF-based Rake receiver. We

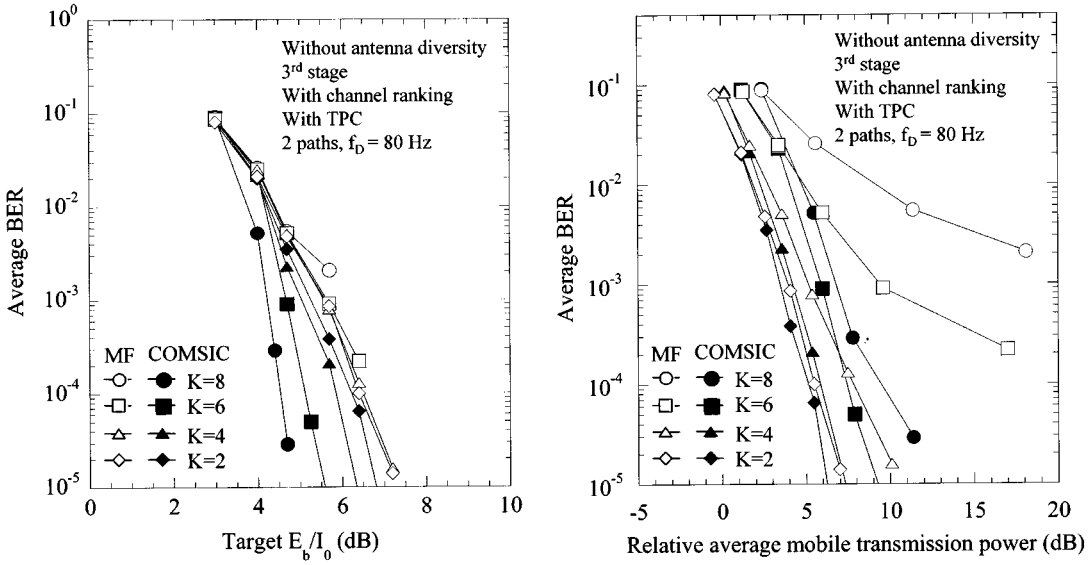

Fig. 16. Average BER performance with the number of active users as a parameter (with TPC, without antenna diversity). (a) Average BER as a function of Target E_b/I_0. (b) Average BER as a function of average mobile transmission power.

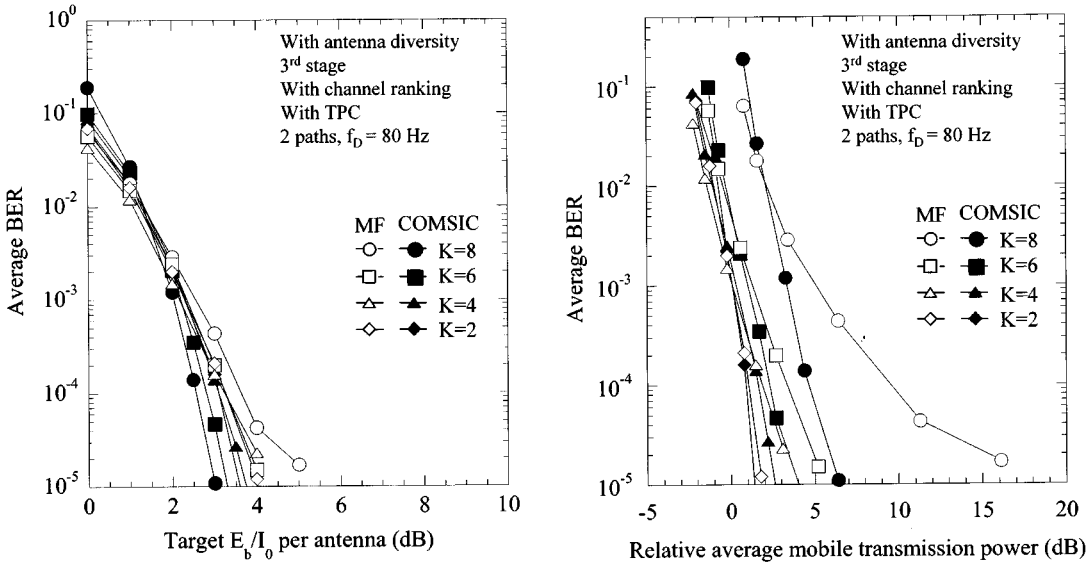

Fig. 17. Average BER performance with the number of active users as a parameter (with TPC, with antenna diversity). (a) Average BER as a function of Target E_b/I_0. (b) Average BER as a function of average mobile transmission power.

emphasize that the results show that the fast TPC with a two-slot delay associated with COMSIC works satisfactorily.

The link capacity is defined as the number of users who can achieve the required BER performance (or total data rate when the data rate of each user is different). Since the average BER is a function of the average SIR or average E_b/I_0, the link capacity is calculated using the average E_b/I_0 required for obtaining the required average BER. In the experiments, the transmission power is normalized by that of the MF-based Rake receiver for a single-user case $(K = 1)$. The measured E_b and N_0 values at the reference transmission power (i.e., 0 dB) were -137.4 dBm/bit/antenna (note that the insertion loss of pilot symbols is included in E_b) and -140 dBm/Hz, respectively. Thus, the received average E_b/N_0 at each transmission power is easily calculated from these two values. The received E_b/I_0 value (note that the background noise power spectrum density is included in I_0) is derived from the relation as

$$E_b/I_0 = E_b \Big/ \left\{ \frac{(K-1/2)E_b}{\mathrm{SF}} + N_0 \right\} = \left\{ \frac{(K-1/2)}{\mathrm{SF}} + \left(\frac{E_b}{N_0} \right)^{-1} \right\}^{-1} \tag{14}$$

where the factor of $1/2$ denotes the multipath interference of the user's own channel since a two-path channel with equal average power is assumed. When the background noise can

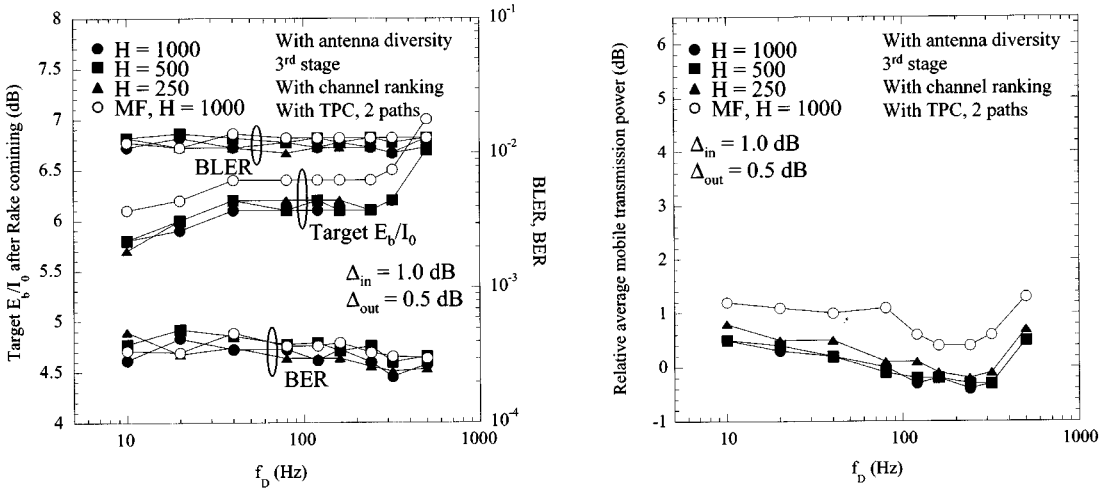

Fig. 18. Effect of FER averaging time on outer loop TPC (with antenna diversity). (a) BLER, BER, and target E_b/I_0. (b) Average mobile transmission power.

be ignored, even if the transmission powers of all active users become half the original transmission powers, the received E_b/I_0 is identical. However, in an actual system, the background noise cannot be ignored. Even in an interference-limited channel, where the background noise is ignored, the impact of the background noise is clearly evident at the COMSIC output. Thus, since the transmission power, i.e., the received E_b/N_0 is decreased, the received E_b/I_0 is decreased [it is clear from (14)]. Fig. 17 also elucidates that when $K = 8$, the transmission power of a MS using COMSIC at the average BER of 10^{-4} is decreased by approximately 3 dB compared with that of the MF-based Rake receiver, thereby the target E_b/I_0 at the identical BER is reduced by approximately 1.0 dB. This indicates that the received E_b/I_0 before interference canceling is decreased by approximately 1.0 dB by employing COMSIC compared with the MF-based Rake receiver because the E_b/I_0 for fast TPC is measured at the MF output, i.e., before interference canceling, in our fast TPC method. Consequently, COMSIC is effective in accommodating a large number of active users with the required quality, that is, in increasing link capacity. In other words, it is beneficial to extend cell coverage while maintaining the same capacity.

2) Performance With Outer Loop Control:

a) Influence of averaging period for BLER measurement: We first investigated the influence of the averaging interval for BLER measurement on the performance when fast TPC with outer loop control is applied. Hereafter, in the evaluations using outer loop, we set the target average BLER to 10^{-2}. The BLER was calculated over H blocks (thus, H frames in the paper). The threshold value, M, which was the number of block errors the CRC results indicated over H blocks, was experimentally optimized so that the average BLER became almost 10^{-2} overall for the f_D region. The average BLER, BER, and target E_b/I_0 performance levels with antenna diversity reception as a function of f_D are plotted in Fig. 18(a) with $\Delta_{\rm in} = 1.0$ dB and $\Delta_{\rm out} = 0.5$ dB. Fig. 18(b) shows the average relative MS transmission power with the same conditions. The MS transmission power was normalized by that for achieving the average BER of 10^{-3} using the COMSIC receiver when $K = 2$ and $f_D = 80$ Hz. Threshold value M of the CRC results for controlling the outer loop control was set to $M = [1, 4, 8]$ for the averaging interval for BLER measurement $H = [250, 500, 1000]$. The figures clearly show that the measured BLER is precisely controlled to the target BLER value over the wide range of f_D from 10 to 500 Hz. It is also evident that the measured BER is also maintained to an almost constant value over the same changes in f_D. The required target E_b/I_0 using COMSIC could be decreased by approximately 1.0 dB at maximum compared with the MF-based Rake receiver with antenna diversity reception when $H = 1000$ due to the interference suppression of COMSIC. From Fig. 18(a), the target E_b/I_0 varies with the variation of approximately 2 dB over the identical range of f_D. The target E_b/I_0 was first increased as the f_D increased up to nearly 80 Hz due to the degradation of tracking performance of fast TPC. As f_D is increased further, the target E_b/I_0 is decreased since the channel coding worked well due to the increasing interleaving effect. However, the target E_b/I_0 is again increased when f_D is greater than 200–300 Hz since the channel estimation with pilot symbols could not track the fast fading variations. As H is increased, the target E_b/I_0 for achieving the identical BLER is decreased because the measurement accuracy of the BLER value is improved. We used the value of $H = 1000$ in the following evaluations since the measured target E_b/I_0 values were saturated at $H = 1000$. Fig. 18(b) shows that the required average MS transmission power with COMSIC is approximately 0.8 dB lower than the case with the MF-based Rake receiver with antenna diversity reception.

We also confirmed by experiments that the optimum parameters in SIR-based fast TPC are identical both in the COMSIC and the MF-based Rake receivers. This is explained as follows. In our proposed fast TPC method, the SIR is measured at the MF output before MAI canceling to eliminate the impact of the successive processing delay in COMSIC employing target E_b/I_0 compensation with outer-loop control. Therefore, the statistical property of the MAI for the SIR measurement is entirely identical for both the COMSIC and the MF-based Rake receivers. In other words, the robustness for the proposed fast

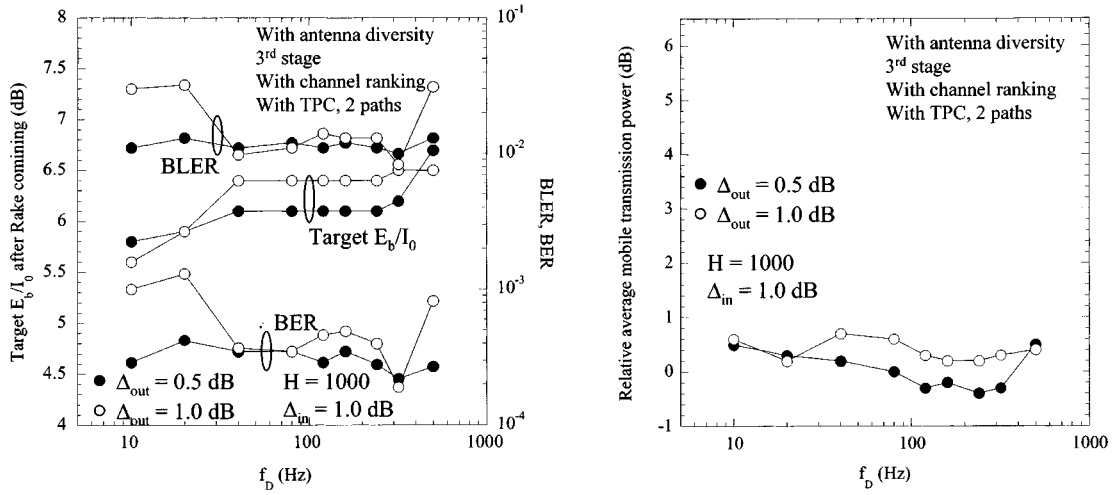

Fig. 19. Effect of $\Delta_{\rm out}$ on outer loop TPC (with antenna diversity). (a) BLER, BER, and target E_b/I_0. (b) Average mobile transmission power.

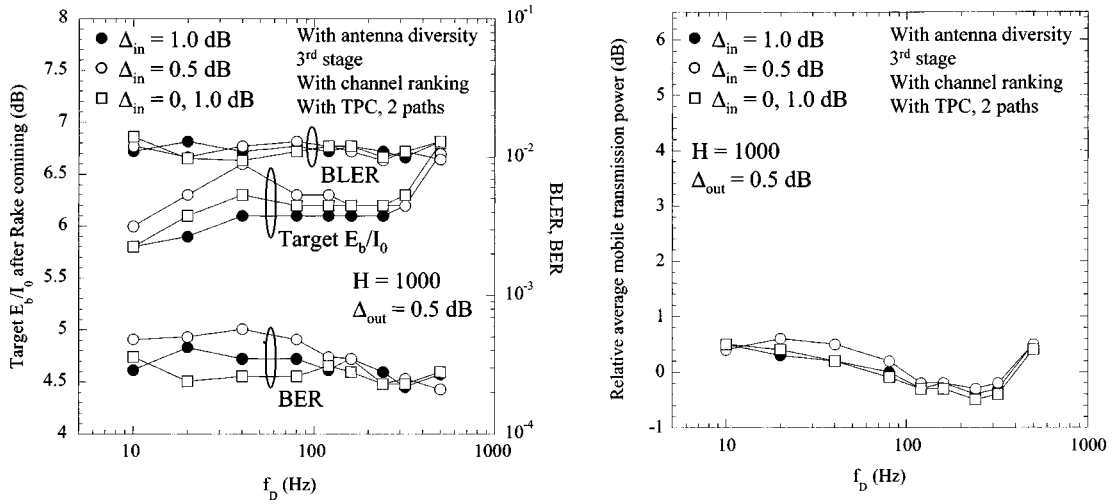

Fig. 20. Effect of $\Delta_{\rm in}$ on outer loop TPC (with antenna diversity). (a) BLER, BER, and target E_b/I_0. (b) Average mobile transmission power.

TPC method that is appropriate for COMSIC is the same as that in the MF-based Rake receiver.

b) Influence of step size of outer loop $\Delta_{\rm out}$: Fig. 19(a) and (b) shows the measured average BLER, BER, and target E_b/I_0 performance, and average MS transmission power performance, respectively, with antenna diversity reception when $\Delta_{\rm out}$ was 0.5 or 1.0 dB with the target $\mathrm{BLER} = 10^{-2}$. It was assumed that $\Delta_{\rm in} = 1.0$ dB and $H = 1000$. The threshold value of M was set to $[7, 7]$. It is found from Fig. 19(a) that the variations of the measured BLER according to the change in f_D increased with $\Delta_{\rm out} = 1.0$ dB compared with the case with $\Delta_{\rm out} = 0.5$ dB. Furthermore, the fluctuation of the controlled target E_b/I_0 value when $\Delta_{\rm out}$ is 1.0 dB becomes larger than that with $\Delta_{\rm out} = 0.5$ dB. Thus, the difference between the assigned target E_b/I_0 value after Rake combining and its real value is increased, resulting in the increase of MS transmission power. The data decision error with $\Delta_{\rm out} = 1.0$ dB occurred more frequently when the target E_b/I_0 is decreased by the outer loop control than that with $\Delta_{\rm out} = 0.5$ dB. This increased the target E_b/I_0 (the target E_b/I_0 is increased by approximately 0.3 dB over the range from $f_D = 20$ to 200 Hz). Fig. 19(b) also indicates that the required MS transmission power with $\Delta_{\rm out} = 0.5$ dB is decreased by approximately 0.2–0.5 dB compared with the case with $\Delta_{\rm out} = 1.0$ dB with antenna diversity reception.

c) Influence of step size of inner loop $\Delta_{\rm in}$: The measured average BLER, BER, and target E_b/I_0 with the inner-loop step size of $\Delta_{\rm in}$ as a parameter without antenna diversity reception are shown in Fig. 20(a), and the corresponding average MS transmission power is also plotted in Fig. 20(b), respectively, with antenna diversity reception. Three types of inner loop controls were evaluated: two-step of $\Delta_{\rm in} = 0.5$ dB and 1.0 dB, and three-step of $\Delta_{\rm in} = 0$ and 1.0 dB. It was assumed that $\Delta_{\rm out} = 0.5$ dB and $H = 1000$ from the previous evaluations. Parameter M was set to $[8, 8, 8]$ for the corresponding inner loop control. Fig. 20(a) shows that the target E_b/I_0 using the two-step control with $\Delta_{\rm in} = 0.5$ dB is increased by approximately 0.5–1.0 dB compared with that with $\Delta_{\rm in} = 1.0$ dB when f_D is lower than 100 Hz, because the inner loop with a small step size can not track the sudden changes in the received signal level due to fading. Three-step size control achieved the same performance as those with the two-step size control using

$\Delta_{\text{in}} = 1.0$ dB. We find from Fig. 20(b) that the required MS transmission power using two-step control with $\Delta_{\text{in}} = 0.5$ dB is increased by approximately 0.3–0.8 dB compared with that with $\Delta_{\text{in}} = 1.0$ dB with antenna diversity reception. The obtained results indicate that the two-step inner loop control with $\Delta_{\text{in}} = 1.0$ dB is appropriate. The results above show that the fast TPC associated COMSIC with outer loop control is very effective in decreasing MS transmission powers in a multipath fading channel in the reverse link.

IV. Conclusion

A three-stage COMSI employing PSA channel estimation for replica generation of MAI was implemented and its performance in frequency selective multipath fading was experimentally evaluated by a multipath fading simulator. A fast TPC method suitable for COMSIC was also proposed, in which SIR at the MF-based Rake receiver is measured to achieve a short TPC delay and the target SIR value is compensated by an outer loop so that the measured BLER is equal to the prescribed target value. The experimental results showed that as expected the COMSIC reduces the MAI satisfactorily even when the number of active users is equal to SF in a multipath fading environment and, thus, improving the BER performance in a multiuser environment. The results also demonstrated that the proposed fast TPC method with a two-slot delay associated with COMSIC works satisfactorily and the combination of COMSIC and fast TPC significantly decrease the transmission power of a mobile station (the required transmission power of a mobile station with COMSIC at the average BER of 10^{-3} is decreased by approximately 2.0 (3.0) dB compared with that with MF-based Rake receiver with (without) antenna diversity reception). This extends the cell coverage and battery life, and increases the system capacity in the reverse link.

Acknowledgment

The authors would like to thank the reviewers for their insightful and constructive suggestions.

References

[1] F. Adachi, M. Sawahashi, and H. Suda, "Wideband DS-CDMA for next generation mobile communications systems," *IEEE Commun. Mag.*, vol. 36, pp. 56–69, Sept. 1998.

[2] E. Dahlman, B. Gudmundson, M. Nilsson, and J. Skold, "UMTS/IMT-2000 based on wideband CDMA," *IEEE Commun. Mag.*, vol. 36, pp. 70–80, Sept. 1998.

[3] K. S. Gilhousen, I. M. Jacobs, R. Padovani, A. J. Viterbi, L. A. Weaver, and C. E. Wheatley III, "On the capacity of a cellular CDMA system," *IEEE Trans. Veh. Technol.*, vol. 40, pp. 303–312, May 1991.

[4] R. Kohno, R. Median, and L. B. Milstein, "Spread spectrum access method for wireless communications," *IEEE Commun. Mag.*, pp. 58–67, Jan. 1995.

[5] AUTHOR NAMES, "TITLE," *Standards Efforts of the ITU, IEEE Personal Commun.*, vol. 4, Aug. 1997.

[6] A. Duel-Hallen, J. Holtzman, and Z. Zvonar, "Multiuser detection for CDMA systems," *IEEE Personal Commun.*, pp. 46–58, Apr. 1995.

[7] S. Moshavi, "Multiuser detection for DS-CDMA communications," *IEEE Commun. Mag.*, pp. 124–136, Oct. 1996.

[8] M. K. Varanasi and B. A. Aazhang, "Multistage detection in asynchronous code-division multiple-access communications," *IEEE Trans. Commun.*, vol. 38, pp. 509–519, Apr. 1990.

[9] Y. C. Yoon, R. Kohno, and H. Imai, "A spread-spectrum multiaccess systems with cochannel interference cancellation for multipath fading channels," *IEEE J. Select. Areas Commun.*, vol. 11, pp. 1067–1075, Sept. 1993.

[10] P. Patel and J. Holtzman, "Analysis of a simple successive interference cancellation scheme in a DS/CDMA system," *IEEE J. Select. Areas Commun.*, vol. 12, pp. 796–807, June 1994.

[11] M. Sawahashi, Y. Miki, H. Ando, and K. Higuchi, "Pilot symbol-assisted coherent multistage interference canceller using recursive channel estimation for DS-CDMA mobile radio," *IEICE Trans. Commun.*, vol. E79-B, pp. 1262–1270, Sept. 1996.

[12] A.-L. Johansson and A. Svensson, "Multistage interference cancellation in multirate DS/CDMA on a mobile radio channel," in *Proc. IEEE VTC*, Apr. 1996, pp. 666–670.

[13] M. Sawahashi, H. Andoh, and K. Higuchi, "Interference replica weight control for pilot symbol-assisted coherent multistage interference canceller using recursive channel estimation in DS-CDMA mobile radio," *IEICE Trans. Commun.*, vol. E81-A, pp. 957–972, May 1998.

[14] S. Parkvall, E. Strom, and B. Ottersten, "The impact of timing errors on the performance of linear DS-CDMA receivers," *IEEE J. Select. Areas Commun.*, vol. 14, pp. 1660–1668, Oct. 1996.

[15] L.-C. Chu and U. Mitra, "Performance analysis of an improved MMSE multiuser receiver for mismatch delay channels," *IEEE Trans. Commun.*, vol. 46, pp. 1369–1380, Oct. 1998.

[16] F. Ling, "Coherent detection with reference-symbol based estimation for direct sequence CDMA uplink communications," in *Proc. VTC'93*, May. 1993, pp. 400–403.

[17] Y. Honda and K. Jamal, "Channel Estimation Based on Time-Multiplexed Pilot Symbols,", IEICE Tech. Rep., RCS96-70, Aug. 1996.

[18] H. Andoh, M. Sawahashi, and F. Adachi, "Channel estimation filter using time-multiplexed pilot channel for coherent rake combining in DS-CDMA mobile radio," *IEICE Trans. Commun.*, vol. E81-B, pp. 1517–1526, July 1998.

[19] K. Higuchi, H. Andoh, K. Okawa, M. Sawahashi, and F. Adachi, "Experimental evaluation of combined effect of coherent rake combining and sir-based fast transmit power control for reverse link of DS-CDMA mobile radio," *IEEE J. Select. Areas Commun.*, vol. 18, pp. 1526–1535, Aug. 2000.

[20] R. Weber, "Low-complexity channel estimation for WCDMA random access," in *Proc. VTC Fall 2000*, Sept. 2000, pp. 344–351.

[21] S. Seo, T. Dohi, and F. Adachi, "SIR-based transmit power control of reverse link for coherent DS-CDMA mobile radio," *IEICE Trans. Commun.*, vol. E81-B, pp. 1508–1516, July 1998.

[22] Y. Amezawa and S. Sato, "A study of SIR measurement methods using signal before rake combining," presented at the 1998 Spring National Convention IEICE Japan, Hiratsuka, Mar. 27–30, 1998.

[23] K. Hamabe, "Outer loop algorithm of transmission power control in CDMA cellular systems," in *Proc. IEICE General Conf.*, B-5-145, Mar. 2001.

Mamoru Sawahashi (M'88) received the B.S. and M.S. degrees from Tokyo University, Japan, in 1983 and 1985, respectively. He received the Dr. Eng. degree from the Nara Institute of Technology, Nara, Japan, in 1998.

In 1985, he joined NTT Electrical Communications Laboratories, Japan. In 1992, he transferred to NTT Mobile Communications Network, Inc., Japan (now, NTT DoCoMo, Inc.). Since joining NTT, he has been engaged in the research of modulation/demodulation techniques for mobile radio, and research and development of wireless access technologies for W-CDMA mobile radio and broadband wireless packet access technologies for beyond IMT-2000. He is now the Director of the Wireless Access Laboratory of NTT DoCoMo, Inc.

Kenichi Higuchi received the B.S. degree from Waseda University, Tokyo, Japan, in 1994.

In 1994, he joined NTT Mobile Communications Network, Inc., Japan (now, NTT DoCoMo, Inc.). Since joining NTT Mobile Communications Network, Inc., he has been engaged in the research and development of code synchronization and interference canceller technique for wideband DS-CDMA mobile radio systems.

Mr. Higuchi is a Member of the Institute of Electronics, Information, and Communication Engineers of Japan.

Hidehiro Andoh received the B.S. and M.S. degrees from Kyusyu Institute of Technology, Fukuoka, Japan.

In 1993, he joined NTT Mobile Communications Network, Inc., Japan (now, NTT DoCoMo, Inc.). Since joining NTT Mobile Communications Network, Inc., he has been engaged in the research and development of coherent RAKE receiving and interference canceller techniques for wideband DS-CDMA mobile radio systems.

Mr. Andoh is a Member of the Institute of Electronics, Information, and Communication Engineers of Japan.

Fumiyuki Adachi (M'79–SM'90–F'01) received the B.S. and Dr. Eng. degrees in electrical engineering from Tohoku University, Sendai, Japan, in 1973 and 1984, respectively.

In April 1973, he joined the Electrical Communications Laboratories of Nippon Telegraph and Telephone Corporation, Japan (now NTT) and conducted various types of research related to digital cellular mobile communications. From July 1992 to December 1999, he was with NTT Mobile Communications Network, Inc. (now NTT DoCoMo, Inc.), where he led a research group on wideband/broadband CDMA wireless access for IMT-2000 and beyond. Since January 2000, he has been at Tohoku University, where he is a Professor of Electrical and Communication Engineering at Graduate School of Engineering. From October 1984 to September 1985, he was a United Kingdom SERC Visiting Research Fellow in the Department of Electrical Engineering and Electronics at Liverpool University. From April 1997 to March 2000, he was a Visiting Professor at Nara Institute of Science and Technology, Japan. His research interests are in OFDM, CDMA, TDMA wireless access techniques, transmit/receive antenna diversity, adaptive antenna array, bandwidth-efficient digital modulation, and channel coding, with particular application to broadband mobile wireless communications systems.

Dr. Adachi served as a Guest Editor of IEEE JOURNAL OF SELECTED AREAS OF COMMUNICATIONS for a special issue on Broadband Wireless Techniques, in October 1999, and for a special issue on Wideband CDMA I, in August 2000. In 1980 and 1990, he was corecipient of the IEEE Vehicular Technology Transactions Best Paper of the Year Award, and a recipient of the Avant Garde Award, in 2000 . He is a member of Institute of Electronics, Information and Communication Engineers of Japan (IEICE) and was a corecipient of the IEICE Transactions Best Paper of the Year Award, in 1996 and 1998.